Tetrahedron 70 (2014) 8914–8918

Contents lists available at ScienceDirect

Tetrahedron

journal homepage: www.elsevier.com/locate/tet

A highly selective and ratiometric fluorescence probe for the detection of Hg^{2+} and pH change based on coumarin in aqueous solution

Shouhai Yang [a], Wenge Yang [b], Qirun Guo [a], Tuan Zhang [a], Keyi Wu [a], Yonghong Hu [a,*]

[a] College of Biotechnology and Pharmaceutical Engineering, Nanjing Tech University, No. 200, North Zhongshan Road, Nanjing 210009, China
[b] Jiangsu Engineering Technology Research Center of Polypeptide Pharmaceutical, Nanjing 210038, China

ARTICLE INFO

Article history:
Received 21 July 2014
Received in revised form 13 September 2014
Accepted 26 September 2014
Available online 2 October 2014

Keywords:
Coumarin
Thioacetal
Fluorescence quenching
Hg^{2+}
pH

ABSTRACT

A simple but highly selective coumarin-based fluorescence probe **1**, 8-(1,3-dithiane)-7-hydroxycoumarin was designed and synthesized for both the ratiometric detection of Hg^{2+} and the on–off response to pH change in aqueous solution. The sensor detected Hg^{2+} selectively via Hg^{2+}-promoted thioacetal deprotection reaction within five minutes and reflected pH in the range from 7.8 to 11.9 as a result of the equilibrium between weak-fluorescent acid form and strong-fluorescent base form. In addition, the probe has an excellent selectivity towards Hg^{2+} over other competitive metal ions for biomedical and environmental applications. The sensing behavior of our probe was studied by UV–visible absorption spectra and fluorescence spectra.

1. Introduction

The detection of ions and molecules by chemosensors is significant for medical diagnostics, analytical chemistry, and biotechnology.[1] Hg^{2+} is known as a severe environmental pollutant because of its durability, which can transfer through biological membranes and accumulate in body, causing damage to health.[2] Considerable efforts have been devoted to the development of Hg^{2+}-selective chemosensors. Among the various chemosensors for Hg^{2+}, fluorescent chemosensors present more advantages: high sensitivity, low cost, and easy detection.[3]

The detection of pH is essential for many processes in agriculture, industry, and human health.[4] As common cations, protons play key roles both in metabolism and cellular events, such as cell growth, calcium regulation, enzyme activities, chemotaxis, and so on.[5] In addition, certain diseases, such as cancers and Alzheimer's disease, have been related to abnormal pH values.[6] Therefore, it is important to be able to measure the intracellular pH promptly and precisely. Interestingly, probe **1** is also sensitive to pH, thus it can be used as a fluorescence probe to measure intracellular pH.

Coumarin is one of the most favorable fluorophore groups to develop fluorescent probes because of its high quantum yields, high photostability, and derivatizable backbone.[7] It was reported that the electron donating groups in the 7-position and electron-withdrawing groups in the 3-position can be able to enhance the fluorescence intensity of coumarins based on an intramolecular charger transfer (ICT) process.[8] In another word, inhibition of such an ICT process may quench the fluorescence.[9] This fluorescence quenching mechanism is involved in our design strategy for the detection.

To the best of our knowledge, there were really few probes with two functions for both metal ions and pH changes.[10] In this work, we described a new probe for rapid, sensitive, selective detection of Hg^{2+} and pH. Our design strategy for the detection took advantage of the well-known specific Hg^{2+}-promoted thioacetal deprotection reaction,[11] which is also a typical off-on emission mode manipulated by acid/base. Thus, probe **1** can be used as one excellent chemosensor for the ratiometric detection of Hg^{2+} and the on–off response to pH.

2. Experimental

2.1. Materials and instruments

7-Hydroxycoumarin was purchased from Aladdin Reagent Co., Ltd and used without purification. Organic solvents purchased from Shanghai Lingfeng chemical reagent Co., Ltd. were all analytical reagent grade. The salts used in stock solutions of metal ions were $NaNO_3$, $Ca(NO_3)_2$, $CdCl_2 \cdot H_2O$, $Co(NO_3)_2 \cdot 6H_2O$, $Mg(NO_3)_2$, $CuSO_4$,

* Corresponding author. Tel./fax: +86 25 83587108; e-mail addresses: yonghonghu11@126.com, 351417841@qq.com (Y. Hu).

http://dx.doi.org/10.1016/j.tet.2014.09.082
0040-4020/

$Zn(NO_3)_2 \cdot 2H_2O$, $Hg(ClO_4)_2$, $Ni(NO_3)_2 \cdot 6H_2O$, $Pb(NO_3)_2$, $AgNO_3$, $CrCl_3 \cdot 6H_2O$, and $FeCl_3$. All of them were of analytical reagent grade and used without purification. Water used in experiment was double distilled water. The UV–visible spectra measurements were performed with a UV–visible spectrophotometer (Unico UV-2800H) equipped with 1.0 cm quartz cells. Fluorescence was recorded on a spectrofluorimeter (Shimadzu RF-5301PC) equipped with 1.0 cm quartz cell. pH values between 4.57 and 12.95 were measured by a PHSJ-4A pH meter (Leichi Ltd., China).

2.2. Synthesis of probe

*2.2.1. Synthesis of probe **1** (8-(1,3-dithiane)-7-hydroxycoumarin).* 1,3-Dimercaptopropane (108 mg, 1 mmol) and boron trifluoride-diethyl etherate (20 μL) were added to a solution of **2** in dichloromethane (5 mL). The yellow solution was stirred overnight at room temperature. After reaction completed, the crude product was purified by flash chromatography (petroleum/ethyl acetate=2:1, v/v) to afford **1** (85.7 mg, yield: 85%). ^{1}H NMR (400 MHz, $CDCl_3$): δ=7.63 (d, J=9.5 Hz, 1H), 7.57 (s, 1H), 7.34 (d, J=8.6 Hz, 1H), 6.87 (d, J=8.6 Hz, 1H), 6.26 (d, J=10.9 Hz, 2H), 3.31–3.09 (m, 2H), 2.93 (dt, J=7.1, 3.8 Hz, 2H), 2.35–2.14 (m, 1H), 2.09–1.84 (m, 1H). ^{13}C NMR (400 MHz, CDCl3) δ 159.75, 159.13, 150.70, 143.02, 128.25, 113.89, 111.65, 111.22, 109.99, 37.98, 30.21, 23.58. ESI-MS: $[M+H]^+$ 281.04 (calcd=281.03), $[M+Na]^+$ 303.01 (calcd=303.01). Elem. Anal. Calcd. for **1**: C 55.69, H 4.31, O 17.12, S 22.87. Found: C 55.57, H 4.42, O 17.04, S 22.97.

Detailed procedures are described in Scheme 1 and characterizations are shown in ESI.

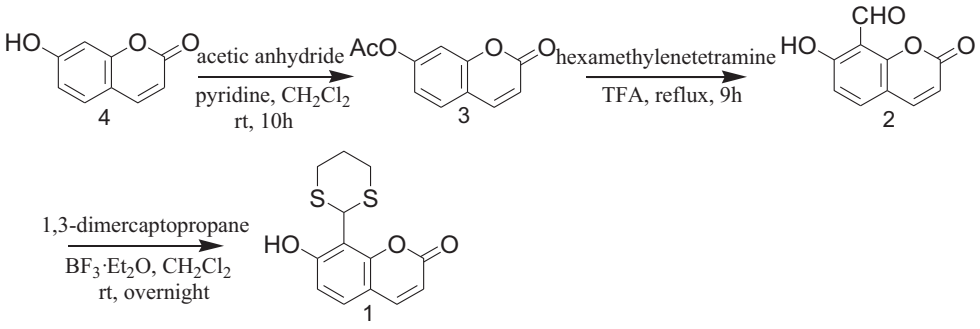

Scheme 1. Synthesis of probe **1**.

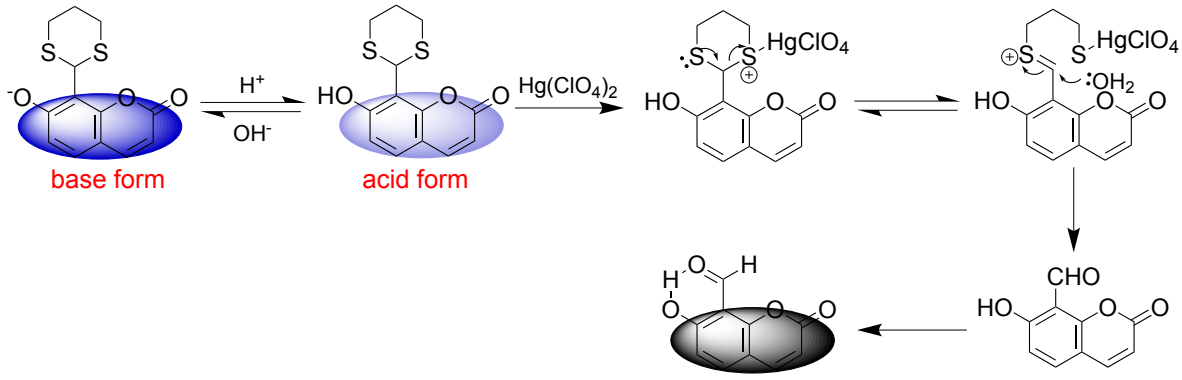

Scheme 2. The response mechanism of probe **1** to Hg^{2+} and pH.

2.3. Preparation of stock solutions

Stock solutions (10 mM) of the anions of Na^+, Ca^{2+}, Cd^{2+}, Co^{2+}, Mg^{2+}, Cu^{2+}, Zn^{2+}, Hg^{2+}, Ni^{2+}, Pb^{2+}, Ag^+, Cr^{3+}, and Fe^{3+} were prepared in ultra-pure water. Stock solutions of **1** (10 μM) were prepared in ethanol aqueous solution (EtOH/H_2O=8:2, v/v). Solutions in the pH range of 4.57–12.95 were prepared by adding the appropriate amounts of NaOH and H_3PO_4. The fluorescence spectra were obtained 5 min after various analytes addition at room temperature by excitation at 385 nm.

3. Results and discussion

3.1. Mechanism of probe 1

The thioacetal group in the 8-position, will be hydrolyzed into aldehyde when Hg^{2+} was added into the system (Scheme 2). The resulting aldehyde forms an intramolecular hydrogen bond with neighboring hydroxyl, thus the original ICT process from the 7-position group to the 8-position group will be inhibited,[12] quenching the fluorescence of probe **1**. In addition, probe **1** with pH-sensitive functional group exists in two forms in different pH solutions: one is the weak-fluorescent acid form, and another is the strong-fluorescent base form (Scheme 2). The equilibrium between these two forms can be adjusted by changing the pH. We can take advantage of the absorption and emission properties to judge the pH value.

3.2. Fluorescence detection of Hg^{2+}

3.2.1. Fluorescence spectral properties. When the excitation was set to 385 nm, probe **1** showed a maximum fluorescence emission peak at 455 nm (Fig. 1). It is noticeable that the stokes shift reaches up to 70 nm, which can effectively overcome background fluorescence, such as the auto-fluorescence from native cellular molecules. Probe **1** showed a maximum fluorescence emission peak at 455 nm without Hg^{2+}. However, upon addition of different concentrations of Hg^{2+}, the peak at 455 nm decreased with increasing the

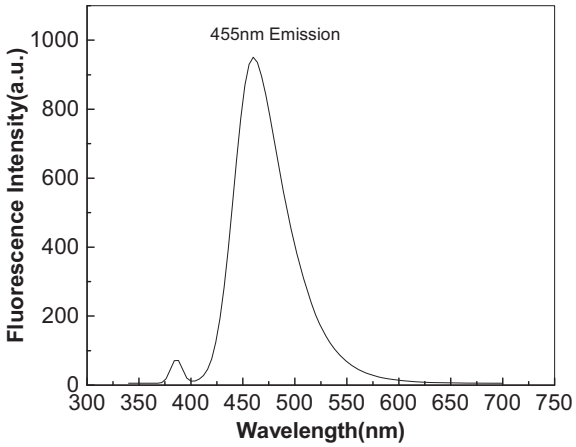

Fig. 1. The fluorescence spectrum of probe **1** at pH=7.

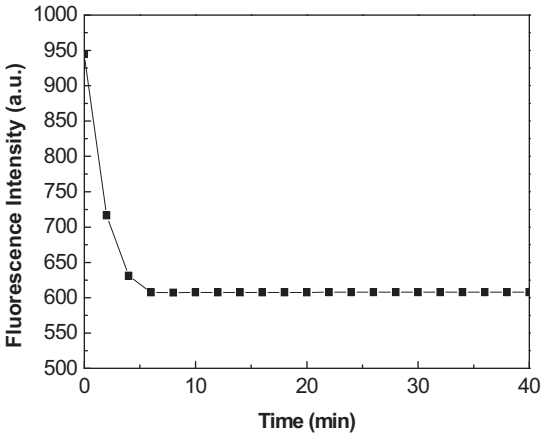

Fig. 3. Fluorescence emission time-course of probe **1** (10 μM) at pH=7 with 1 equiv Hg^{2+} in EtOH/H_2O (v/v=8/2).

concentration of Hg^{2+} (Fig. 2A). Moreover, there was a good linearity obtained between the fluorescence intensity (a.u.) with the Hg^{2+} concentration ranging from (0–3)*10^{-5} mM (Fig. 2B). The linear equation is $y=-185.416x+850.33$ ($R^2=0.9957$), where x, y represents the concentration of Hg^{2+} (mM) and the fluorescence intensity, respectively. All properties mentioned above indicate the capability of probe **1** for quantitatively detecting Hg^{2+} by a ratiometric fluorescence method.

probe **1** toward Hg^{2+} is unaffected by the presence of the other possible contaminating metal ions, demonstrating that probe **1** could meet the selective requirements for biomedical and environmental applications.

3.3. UV–visible and fluorescence response to pH

The UV–visible and fluorescence titrations were performed at a probe concentration of 10 μM. As shown in Fig. 5A, probe **1**

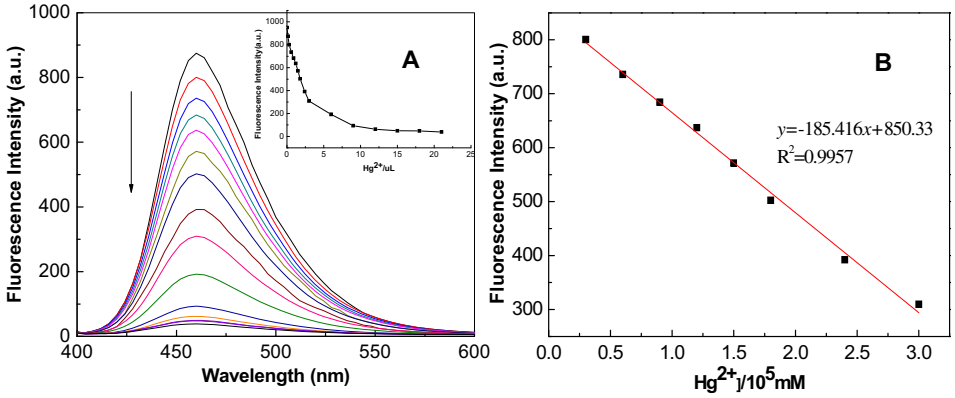

Fig. 2. A: Fluorescence response (λ=455 nm) of 3 mL (10 μM) probe **1** at pH=7 to Hg^{2+} volume of 0, 0.15, 0.3, 0.6, 0.9, 1.2, 1.5, 1.8, 2.4, 3, 6, 9, 12, 15, 18, and 21 μL (10 mM) in EtOH/H_2O (v/v=8/2), respectively. B: Fluorescence intensity as a function of Hg^{2+} concentration.

3.2.2. Influence of reaction time. In order to understand how **1** – Hg^{2+} system changed with time, the time-dependent fluorescence spectra of probe **1** in the presence and absence of Hg^{2+} were studied. As shown in Fig. 3, upon addition of Hg^{2+}, the fluorescence intensity (a.u.) reduced gradually along with the time consuming. The minimum was reached after about 5 min and then the fluorescence intensity (a.u.) remains stable. Thus, probe **1** could be used for rapid detection of Hg^{2+}.

3.2.3. Selectivity. In order to enable the probe to work in more complex systems, we studied the selectivity and competition under the same condition, which is one of the most important performance indexes for the detection of Hg^{2+}.[13] Na^+, Ca^{2+}, Cd^{2+}, Co^{2+}, Mg^{2+}, Cu^{2+}, Zn^{2+}, Hg^{2+}, Ni^{2+}, Pb^{2+}, Ag^+, Cr^{3+}, and Fe^{3+} were selected as competing ions and introduced into the detecting system. In Fig. 4, the black bar portion shows that our proposed probe exhibits high selectivity toward Hg^{2+} over other metal ions. Furthermore, the red bar portion indicates that the response of the

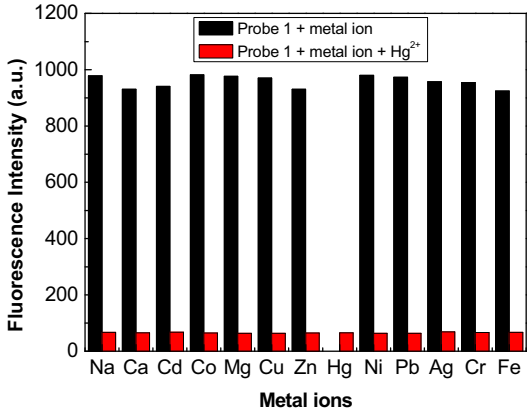

Fig. 4. Fluorescence spectral data of 3 mL (10 μM) probe **1** at pH=7.0 with 4 equiv metal ions Na^+, Ca^{2+}, Cd^{2+}, Co^{2+}, Mg^{2+}, Cu^{2+}, Zn^{2+}, Hg^{2+}, Ni^{2+}, Pb^{2+}, Ag^+, Cr^{3+}, and Fe^{3+} in EtOH/H_2O (v/v=8/2).

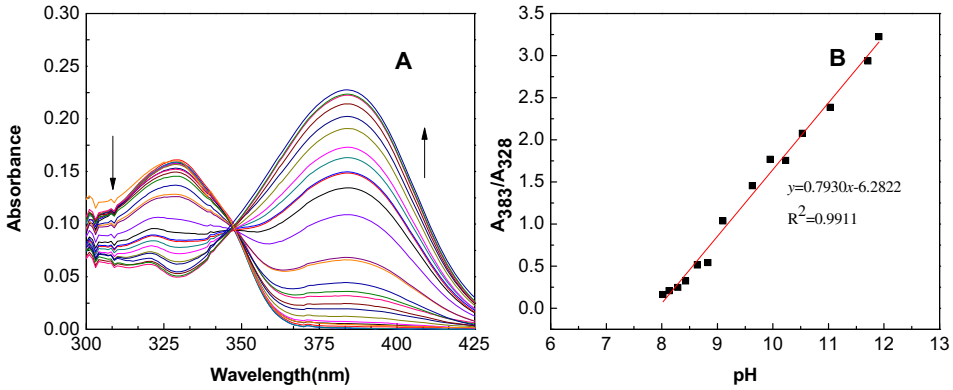

Fig. 5. A: Changes of the UV–visible absorption spectra of probe **1** (10 μM) with pH increase from 4.57 to 12.95 in EtOH/H_2O (v/v=8/2). B: Absorption intensity ratio A_{383}/A_{328} of probe **1** as a function of pH.

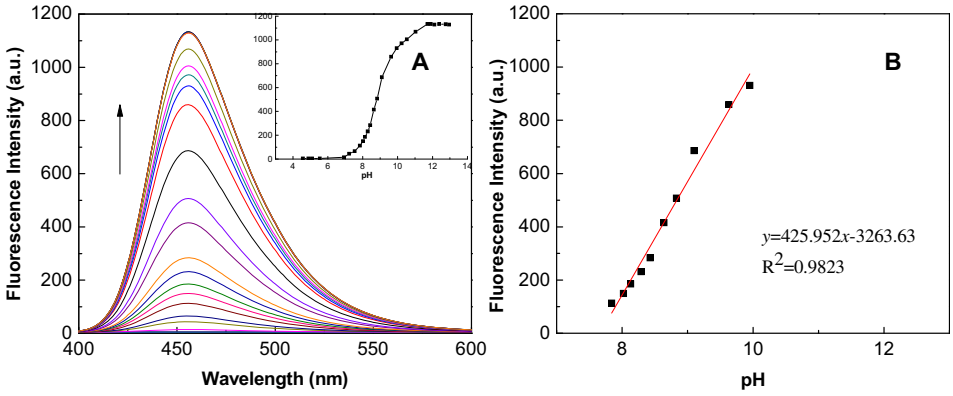

Fig. 6. A: Changes of the fluorescence intensity (a.u.) of probe **1** (10 μM) with pH increasing from 4.57 to 12.95 in EtOH/H_2O (v/v=8/2). B: Fluorescence intensity (a.u.) of probe **1** as a function of pH.

displayed typical pH-dependent UV–visible absorption behavior. As pH increased from 4.57 to 12.95, the absorption band centered at 328 nm decreased gradually while a new peak simultaneously appeared at 383 nm. The obvious isosbestic point at 347 nm was observed from Fig. 5A, which indicates the presence of acid–base equilibrium between the two forms of probe **1** (Scheme 2). What's more, the ratio of fluorescence intensity between 383 nm and 328 nm (F_{383}/F_{328}) changes from 0.164 to 3.225 (R=19.7 fold). There was a linearity between the F_{383}/F_{328} and pH ranging from 8.02 to 11.91, and the linear equation is y=0.7930x–6.2822 (R^2=0.9911), where x, y represents pH and the fluorescence intensity, respectively (Fig. 5B).

The fluorescence spectra of probe **1** at various pH values were shown in Fig. 6A. With the pH value of test solution increasing, a significant fluorescence turn-on response is noted in the emission spectra. A good linearity (R^2=0.982) between fluorescence and pH ranging from 7.84 to 9.95 was obtained according to fluorescence titration (Fig. 6B). The analysis of fluorescence intensity changes as a function of pH by using the Henderson–Hasselbalch-type mass action Eq. 1 yielded a pKa of 8.92:

$$\lg[(F_{max}-F)/(F-F_{min})] = pKa - pH \quad (1)$$

where F is the fluorescence emission intensity at 455 nm. It means that probe **1** can serve as a functional pH probe that might work for basic organelles.

4. Conclusion

In summary, we have designed and synthesized a highly selective and ratiometric dual-functional fluorescence probe **1** with advantages as follows: (1) Probe **1** can be used for the ratiometric detection of Hg^{2+} within 5 min; (2) The stokes shift reaches up to 70 nm, which can effectively overcome background fluorescence; (3) Probe **1** is highly selective for Hg^{2+} over the other competing metal ions; (4) In addition to the detection of Hg^{2+}, it can also serve as an outstanding pH probe (pH 7.8–11.9) that might work for basic organelles.

Acknowledgements

This work was financially supported by the National High Technology Research and Development Plan (2011AA100901), the Science and Technology Support Program—Agriculture Part (BE2013442), the Joint Innovation and Research Funding-Prospective Joint Research Projects (SBY201320243), the Doctoral Fund Class Topics (2011322111000).

Supplementary data

Supplementary data related to this article can be found at http://dx.doi.org/10.1016/j.tet.2014.09.082.

References and notes

1. (a) Ding, W. H.; Cao, W.; Zheng, X. J. *Dalton Trans.* **2014**, *43*, 6429–6435; (b) Weerasinghe, A. J.; Schmiesing, C.; Sinn, E. *Tetrahedron Lett.* **2009**, *50*, 6407–6410; (c) Shellaiah, M.; Wu, Y. H.; Lin, H. C. *Analyst* **2013**, *138*, 2931–2942; (d) Yuan, M. J.; Zhou, W. D.; Liu, X. F. *J. Org. Chem.* **2008**, *73*, 5008–5014.
2. (a) Zhu, B. C.; Wang, W. Z.; Liu, L. Y. *Sens. Actuators, B* **2014**, *191*, 605–611; (b) Aksuner, N.; Basaran, B.; Henden, E. *Dyes Pigm.* **2011**, *88*, 143–148; (c) Järup, L. *Br. Med. Bull.* **2003**, *68*, 167–182; (d) Zhu, M.; Yuan, M. J.; Liu, X. F. *Org. Lett.* **2008**, *10*, 1481–1484.

3. (a) Núñez, C.; Diniz, M.; Dos Santos, A. A. *Dyes Pigm.* **2014**, *101*, 156–163; (b) Shi, J.; Wang, Y.; Tang, X. *Dyes Pigm.* **2014**, *100*, 255–260; (c) Yuan, M. J.; Li, Y. L.; Li, J. B. *Org. Lett.* **2007**, *9*, 2313–2316.
4. Kordac, M.; Linek, V. *Ind. Eng. Chem. Res.* **2008**, *47*, 1310–1317.
5. Ma, L.; Cao, W.; Liu, J. *Sens. Actuators, B* **2012**, *169*, 243–247.
6. (a) Davies, T. A.; Fine, R. E.; Johnson, R. J. *Biochem. Biophys. Res. Commun.* **1993**, *104*, 537–543; (b) Izumi, H.; Torigoe, T.; Ishiguchi, H. *Cancer Treat. Rev.* **2003**, *29*, 541–549.
7. (a) Dai, X.; Wu, Q. H.; Wang, P. C. *Biosens. Bioelectron.* **2014**, *59*, 35–39; (b) Mahapatra, A. K.; Maiti, K.; Sahoo, P. *J. Lumin.* **2013**, *143*, 349–354; (c) Zhou, Z.; Li, N.; Tong, A. *Anal. Chim. Acta* **2011**, *702*, 81–86.
8. (a) Setsukinai, K.; Urano, Y.; Kikuchi, K. *J. Chem. Soc., Perkin Trans. 2* **2000**, *12*, 2453–2457; (b) Ezeh, V. C.; Harrop, T. C. *Inorg. Chem.* **2013**, *52*, 2323–2334.
9. Long, L.; Zhou, L.; Wang, L. *Org. Biomol. Chem.* **2013**, *11*, 8214–8220.
10. (a) YoungáNoh, J.; JináPark, G.; JeongáNa, Y. *Dalton Trans.* **2014**, *43*, 5652–5656; (b) Ramasamy, K.; Thambusamy, S. *J. Lumin.* **2014**, *149*, 12–18.
11. (a) Mahapatra, A. K.; Maji, R.; Sahoo, P. *Tetrahedron Lett.* **2012**, *53*, 7031–7035; (b) Lu, F.; Yamamura, M.; Nabeshima, T. *Dalton Trans.* **2013**, *42*, 12093–12100.
12. (a) Lee, K. S.; Kim, H. J.; Kim, G. H. *Org. Lett.* **2008**, *10*, 49–51; (b) Albayrak, C.; Odabasoglu, M.; Buyukgungor, O. *Acta Crystallogr., Sect. C* **2004**, *60*, 318–320.
13. (a) Liu, Y. W.; Chen, C. H.; Wu, A. T. *Analyst* **2012**, *137*, 5201–5203; (b) Sarkar, S.; Roy, S.; Sikdar, A. *Analyst* **2013**, *138*, 7119–7126.